Characterization of the Role of the Stimulatory Magnesium of *Escherichia coli* Porphobilinogen Synthase†

Eileen K. Jaffe,* Shafinaz Ali, Laura W. Mitchell, Kathleen M. Taylor, Marina Volin, and George D. Markham

Institute for Cancer Research, Fox Chase Cancer Center, 7701 Burholme Avenue, Philadelphia, Pennsylvania 19111

Received April 8, 1994; Revised Manuscript Received August 11, 1994®

ABSTRACT: The synthesis of tetrapyrroles is essential to all phyla. Porphobilinogen synthase (PBGS) is a zinc metalloenzyme that catalyzes the formation of porphobilinogen, the monopyrrole precursor of all biological tetrapyrroles. The enzyme from various organisms shows considerable sequence conservation, suggesting a common fold, quaternary structure, and catalytic mechanism. *Escherichia coli* and plant PBGS are activated by magnesium, a property that is absent from mammalian PBGS. This stimulatory Mg(II) is called Mg_C. Mg_C is not required for activity and is distinct from the two zinc ions (Zn_A and Zn_B) common to mammalian and *E. coli* PBGS ($PBGS_{E.\ coli}$). For $PBGS_{E.\ coli}$, both the K_m for the substrate 5-aminolevulinic acid (ALA) and the V_{max} are altered by the presence of Mg_C; Mg(II) causes the K_m to drop from ~3 to 0.30 mM and the maximum specific activity to increase from 23 to 50 μmol h^{-1} mg^{-1}. Mg_C also causes the saturating concentration of the required Zn(II) to decrease from 0.1 mM to 10 μM. Maximal activation by Mg(II) occurs at 0.5 mM; thus, in *E. coli* the Mg_C site is probably saturated under physiological conditions. Mn(II) is a good substitute for Mg_C, giving a comparable increase in catalytic activity. Consequently, Mn(II) has been used as an EPR active probe of the Mg_C binding site. Mn(II) binds at a stoichiometry of eight ions per enzyme octamer. The X- and Q-band EPR spectra reflect a single type of binding site with rhombic symmetry and are consistent with oxygen and/or nitrogen ligands. The addition of unlabeled or 1-^{13}C-labeled ALA does not significantly affect the Mn(II) EPR spectra. The Mg_C binding sites apparently are distant from each other and also distant from the active sites. The eight equivalent Mg_C's of $PBGS_{E.\ coli}$ are in sharp contrast to the four active sites. Mg_C has a profound effect on the quaternary structure of the protein. $PBGS_{E.\ coli}$ octamers dissociate into smaller species during native gel electrophoresis. Preincubation of the protein in EDTA potentiates the dissociation, while preincubation of the protein in Mg(II) or Mn(II) and/or ALA hinders dissociation. Two-dimensional electrophoresis experiments demonstrate that the protein can reassemble within the gel to form octamers upon incubation with Mg(II) and/or ALA. Catalytic activity is observed for all species within the gel. Since assay conditions promote octamer formation, it is not possible to determine whether smaller species are active.

The metalloprotein porphobilinogen synthase (PBGS)[1] catalyzes the asymmetric condensation of two molecules of 5-aminolevulinate (ALA) to form porphobilinogen (PBG), the common precursor of porphyrins, corrins, chlorins, and other tetrapyrroles (Shemin & Russell, 1954). Thirteen amino acid sequences for PBGS from mammals, fungi, plants, non-photosynthetic bacteria, methanogenic bacteria, and nitrogen-fixing bacteria have been documented (Wetmur et al., 1986; Bishop et al., 1986; 1989; Myers et al., 1987; Li et al., 1989; Echelard et al., 1988; Boese et al., 1991; Schaumburg et al., 1992; Hannson et al., 1991; Bröckl et al., 1992; Chauhan & O'Brian, 1993; Lingner & Kleinschmidt, 1983; Jaffe et al., 1992; Markham et al., 1993; Kaczor et al., 1994). There is high conservation among PBGS amino acid sequences from all of these species (23% identity, 38% similarity), which covers all but the most N-terminal region (see Figure 1). This conservation suggests that the protein fold, quaternary structure, and fundamental catalytic mechanism are conserved through evolution. Nevertheless, there are species-dependent differences in PBGS metal ion usage and metal ion requirements for enzyme activity that have caused previous workers to discriminate the PBGSs along phylogenetic lines (Shemin, 1972; Jordan, 1991). In fact, using this phylogenetic classification, the known PBGSs can be described in terms of three functionally distinct metal ion binding sites, A, B, and C, as illustrated in Table 1. The species-dependent variation in metal activation is described in the following paragraphs and in the Discussion section.

Mammalian PBGS contains two types of Zn(II), denoted Zn_A and Zn_B (binding at sites A and B, respectively). These Zn(II)'s have been discriminated both functionally (Jaffe et al., 1992, 1994) and by extended X-ray absorption fine structure spectroscopy (EXAFS) (Dent et al., 1990). Zn_A and Zn_B each are present at a stoichiometry of four per octamer, or eight Zn(II)'s in all (Jaffe et al., 1992; Dent et al., 1990). Zn_A is essential to catalysis and has been proposed to play a role in inter-ALA bond formation (Jaffe et al., 1992). Because of its essential role in catalysis, Zn_A

† This work was supported by NIH Grants ES03654 (E.K.J.), CA06927, and CA09035 (FCCC) and by an appropriation from the Commonwealth of Pennsylvania. Its contents are solely the responsibility of the authors and do not necessarily represent the official views of the National Cancer Institute.

* Author to whom correspondence should be addressed.

® Abstract published in *Advance ACS Abstracts,* December 1, 1994.

[1] Abbreviations: PBGS, porphobilinogen synthase (5-aminolevulinate dehydratase); ALA, 5-aminolevulinate; PBG, porphobilinogen; EXAFS, extended X-ray absorption fine structure spectroscopy.

0006-2960/95/0434-244$09.00/0

TDLIQRPRRLRKSPALPRMFEETTLSLNDLVLPIFVEEEIDDYKAVEA 48
MPGVMRIPEKHLAREIERIANAGIRSVMTFGISHHTDETGSDAW 92
REDGLVARMSRICKQTVPEMIVMSDTCFCEYTSHGHCGVLCE 134
HGVDNDATLENLGKQAVVYAAAGADFIAPSAAMDGQVQ 172
AIRQALDAAGFKDTAIMSYSAKFASSFYGPFREAAGSA 210
LKGDRKSYQMNPMNRAEGIAEYLLDEAQGADCLMVK 246
PAGAYLDIVRELRERTELPIGAYQVSGEYAMIKFAALA 284
GAIDEEKVVLESLGSIKRAGADLIFSYFALDLAEKKILR 323

FIGURE 1: Highly conserved PBGS sequence. Thirteen phylogenetically diverse PBGS sequences are documented. The $PBGS_{E.\ coli}$ sequence is illustrated. Large single-letter codes are used for amino acids that are identical in at least 12 of the 13 sequences. Medium-sized letters are used for amino acids that show highly conservative substitutions. Small letters are used for all other amino acids. Underlined large type amino acids indicate positions where the *E. coli* sequence is the one out of thirteen that is not identical.

Table 1: A Three-Metal-Ion Model for PBGS

species	site A[a]	site B[b]	site C[c]	total metal ions
mammalian and yeast	4 Zn	4 Zn		8
E. coli and perhaps other bacteria	4 Zn	4 Zn	8 Mg	16
plant and perhaps other bacteria	4 Zn	4 Mg	8 Mg	16

[a] Essential for activity, most tight binding, predominantly O and N ligands; not yet proven for plant PBGS where the K_d is expected to be very tight. [b] Zn_B is not essential for mammalian PBGS when assayed in the presence of 2-mercaptoethanol. Zn_B may be essential for $PBGS_{E.\ coli}$ activity. Mg_B has been proposed to be essential wherever it occurs (Jaffe et al., 1994). See Figure 2 for the putative B site metal binding motif. [c] A putative Mg_C binding site has been proposed (Mitchell & Jaffe, 1993); see Figure 3. The identity and stoichiometry of the Mg_C sites are established in this paper.

has been proposed to be common to PBGS from all species (see Table 1). EXAFS analysis shows that Zn_A is pentacoordinate and has predominantly oxygen and nitrogen ligands, while Zn_B has four cysteine ligands (Dent et al., 1990). Recent studies have suggested that the B site is also located at the active site (Jaffe et al., 1994). Zn_B is not essential to the activity of mammalian PBGS when assays are carried out in the presence of 2-mercaptoethanol. A four-cysteine cluster common to mammalian, yeast, and some bacterial PBGSs is the likely binding site for Zn_B (Markham et al., 1993; Jaffe, 1993) (see Figure 2). This putative zinc binding site was first identified as a cysteine and histidine containing "zinc finger-like" region in the human PBGS sequence (Wetmur et al., 1986). The common dogma that frequently cites this region as the binding site for *all* Zn(II)'s of PBGS, including Zn_A, is undoubtedly an oversimplification [*e.g.*, see Spencer and Jordan (1993)]. Mammalian PBGS does not appear to use a third divalent metal ion.

Escherichia coli PBGS ($PBGS_{E.\ coli}$) has been shown to require Zn(II) for activity (Mitchell & Jaffe, 1993; Spencer & Jordan, 1993), and the protein sequence contains the proposed binding sites for Zn_A and Zn_B as found in mammalian PBGS (Jaffe, 1993). The Zn EXAFS of $PBGS_{E.\ coli}$ with eight Zn(II)'s per octamer is very similar to that of bovine PBGS.[2] Mg(II) is not required for activity, but stimulates the maximal velocity of $PBGS_{E.\ coli}$ (Mitchell & Jaffe, 1993; Spencer & Jordan, 1993). Mg(II) does not stimulate mammalian PBGS activity. In the presence of

[2] S. Hasnain, R. Strange, L. W. Mitchell, and E. K. Jaffe, unpublished results.

human NLLVACDVCLCPYTSHGHCGLLSEN
rat TLLVACDVCLCPYTSHGHCGLLSEN
mouse SLLVACDVCLCPYTSHGHCGLLSEN
bovine SLLVACDVCLCPYTSHGHCGLLSEN
yeast ELYIICDVCLCEYTSHGHCGVLYDD
E.coli EMIVMSDTCFCEYTSHGHCGVLCEH
B.subtilus EMVVVADTCLCEYTDHGHCGLVK.D
M.sociabilis DLVVITDVCLCQYTEHGHCGIVK.N
B.japonicum EIGVLCDVALDPFTSHGHDGLI.AD
pea DLIIYTDVALDPYSSDGHDGIVRED
soybean DLVIYTDVALDPYSSDGHDGIVRED
moss DLVIYTDVALDPYSSDGHDGIVRED
spinach DLIIYTDVALDPYYYDGHDGIVTQH

FIGURE 2: Putative B site metal binding region. Cysteines, histidines, and acidic residues are emphasized. Zn_B has been shown to bind to four cysteine residues in bovine PBGS (Dent et al., 1990) and has been proposed to bind to this continuous sequence (Jaffe, 1993). The illustrated region of PBGS was first identified as a putative Zn(II) binding region by homology to the now classic cysteine- and histidine-containing zinc finger (Wetmur et al., 1986). Four cysteines are present in this region of PBGS from mammals, yeast, and *E. coli*. This region of plant PBGS is devoid of cysteines, rich in aspartic acids, and proposed to be a Mg(II) binding site (Boese et al., 1991). It is now denoted the Mg_B binding site. *Bradyrhizobium japonicum* PBGS contains an interesting hybrid sequence in this region (Chauhan & O'Brian, 1993); its metal ion requirements are currently under investigation.

mouse LPPGARGLALRAVAR
rat LPPGARGLALRAVAR
human LPPGARGLALRAVDR
bovine LPPGARGLALRAVDR
yeast LPPAGRGLARRALER
B.japonicum MDSANTDEALREVEL
B.subtilus MDPANRMEALREAQS
M.sociabilis MDPPNSLEALREVKL
E.coli MNPMNRAEGIAEYLL
moss MNPANYREALLEVHA
spinach MNPANYREALIETQE
pea MNPANYREALTEMRE
soybean MNPANYREALTEMRE

FIGURE 3: Putative nucleus for Mg_C binding. To identify potential ligands to Mg_C, the $PBGS_{E.\ coli}$ sequence was examined for residues similar to plant PBGS and significantly different from mammalian PBGS, since mammalian PBGS has no Mg_C. This region of bacterial and plant PBGS is rich in oxygen- and nitrogen-containing side chains (emphasized) that are absent from mammalian and yeast PBGS. Although no data point to a continuous Mg_C binding site, most metal ions bound to proteins are ligated through a nucleus of at least two nearby residues. Consequently, this region was identified as a potential Mg_C nucleation site (Mitchell & Jaffe, 1993).

saturating amounts of Mg(II), $PBGS_{E.\ coli}$ binds Zn(II) at a stoichiometry of eight per octamer (Spencer & Jordan, 1993), which is equivalent to the sum of Zn_A and Zn_B binding sites in mammalian PBGS (Jaffe et al., 1992; Dent et al., 1990). In the absence of Mg(II), $PBGS_{E.\ coli}$ binds Zn(II) at a stoichiometry of 16 per octamer (Spencer & Jordan, 1993; Mitchell & Jaffe, 1993), suggesting that Zn(II) can occupy the Mg(II) site with different functional consequences. Plant PBGS exhibits a similar stimulation of activity upon the addition of Mg(II) (Prasad et al., 1988; Shibata & Ockiai, 1977), but the stoichiometries of metal ions bound to plant PBGS have not as yet been determined. We have compared the sequence of $PBGS_{E.\ coli}$ with mammalian and plant PBGSs and predicted a region of the sequence that might form part of the binding site for the stimulatory Mg(II), hereafter called Mg_C (Mitchell & Jaffe, 1993) (see Figure 3). The putative

Mg_C binding site is distinct from the binding sites for Zn_A or Zn_B.

The focus of the present report is the characterization of the Mg_C of $PBGS_{E.\ coli}$. Mg_C has been found to dramatically reduce the value of K_m of $PBGS_{E.\ coli}$ for ALA, increase the V_{max}, and lower the minimal saturating concentration of Zn(II). One striking observation is that Mg_C stabilizes the quaternary structure of the *E. coli* protein. Functional studies show that the paramagnetic Mn(II) ion substitutes well for Mg_C. Consequently, EPR spectroscopy of the Mn(II)−enzyme complex has been used to quantify and characterize the binding sites for the C ion.

EXPERIMENTAL PROCEDURES

Materials. Aminolevulinic acid (ALA) hydrochloride, monobasic potassium phosphate (KP_i), *N*-[tris(hydroxymethyl)methyl]-2-aminoethanesulfonic acid (TES), and *p*-(dimethylamino)benzaldehyde, were purchased from Sigma Chemical Co. 2-Mercaptoethanol (βME) was purchased from Fluka Chemical Corp. and distilled under vacuum prior to use. $HgCl_2$, $ZnCl_2$, $MgCl_2$ (ultrapure), and high-purity KOH were purchased from Aldrich Chemical Co. Centrifree and Centriprep ultrafiltration devices were purchased from Amicon Corp. Trifluoroacetic acid was purchased from Pierce. House-distilled water was further purified by passage through a Milli-Q water purification system (Millipore). [1-^{13}C]ALA was custom-synthesized by MSD (now C.D.N.) Isotopes. All other chemicals were reagent grade.

Enzyme Purification, Assay, and Kinetic Characterization. $PBGS_{E.\ coli}$ was purified as previously described (Mitchell & Jaffe, 1993), with the exception that 10 μM Mg(II) was included in all purification buffers.[3] PBGS activity assays, as well as K_m and V_{max} determinations, were as previously described (Mitchell & Jaffe, 1993). In most cases the assay buffer contained 0.1 M potassium phosphate (pH 7.0) and 10 mM βME. For the assays illustrated in Figure 1, the assay was started by the addition of ALA-HCl to a final concentration of 10 mM, which lowered the pH to 6.8. The concentrations of Mg(II) and Zn(II) are as described in the figure legends or elsewhere in the text. For the determination of kinetic constants, the final pH of the assay was controlled by adding HCl such that the added ALA-HCl plus HCl equaled 10 mM. To avoid complications due to Mn(II) phosphate complexes, studies with Mn(II) used the buffer 0.1 M TES−KOH (pH 7.0), with 30 μM Zn(II) and 10 mM βME added.

Gel Electrophoresis and Activity Staining. One- and two-dimensional native gels and one-dimensional SDS gels were run on a Pharmacia PhastGel system using 12.5% acrylamide gels. Following electrophoresis, native PhastGels were placed in 7 mL of 0.1 M KP_i (pH 7), 10 mM βME, and 30 μM Zn, with or without 1 mM $MgCl_2$, and preincubated at 37 °C for 0−10 min. ALA-HCl was added to a final concentration of 6 mM. Following incubations that varied from 10 min to 1 h, the gels were incubated in 3 mL of 0.1 M $HgCl_2$ and 20% trichloroacetic acid at room temperature for ~2 min, after which time PBG was detected by the pink color that appeared after the gels were placed in 3 mL of modified Ehrlich's reagent (Mauzerall & Granick, 1956). Photographs were taken within 10−15 min of addition of Ehrlich's reagent. After the activity stains were complete, the same gels were soaked in 20% TCA for 1 h and stained for protein. SDS PhastGels and native PhastGels, which were not activity-stained, were stained for protein per standard PhastGel protocol.

Mn(II) EPR Spectroscopy. X-band (9.12 GHz) EPR spectra were obtained on a computer-interfaced Varian E-109 spectrometer. Binding studies were performed at 21 °C; single scans were recorded with spectrometer settings of 10 mW microwave power, 12.5 G modulation amplitude, and a sweep rate of 4 G/s. Spectra of enzyme-bound Mn(II) were obtained at 4 °C with spectrometer settings of 100 mW microwave power, 10 G modulation amplitude, and a sweep rate of 8 G/s; four scans were averaged. Q-band (33.8 GHz) spectra were obtained on a Bruker ER200D spectrometer. Single scans were recorded at 225 K using spectrometer settings of 100 mW microwave power, 5 G modulation amplitude, and a 12 G/s sweep rate.

To establish that Mg(II) displaces enzyme-bound Mn(II), EPR spectra were obtained for samples containing 0.2 mM $PBGS_{E.\ coli}$ subunits, 50 μM Mn(II), 0.1 M TES−KOH (pH 7), 30 μM Zn(II), and 10 mM βME in the presence and absence of Mg(II) (1 and 5 mM). A solution of 50 μM Mn(II) in protein-free buffer was the sample for a control spectrum.

Q-band spectra of the enzyme−Mn(II) complex were simulated using a computer program that uses a third-order perturbation theory treatment of the Mn(II) spin Hamiltonian (Reed & Markham, 1984); the underlying assumptions of this treatment often are not valid for the analysis of X-band spectra. The Mn(II) ion has five unpaired electrons, and the 100% abundant ^{55}Mn nucleus is spin 5/2. The parameters to be garnered from simulations include the following: the electron−nuclear hyperfine coupling constant, *A*, which describes the magnitude of the interaction between the unpaired electrons and the Mn nuclear spin, and the two zero field splitting parameters, *D* and *E/D*, which reflect the deviation of the coordination sphere from cubic and axial symmetry, respectively (Reed & Markham, 1984). The values of *E/D* can range from 0 for axial symmetry to 1/3 for totally rhombic symmetry.

For determination of the stoichiometry of Mn(II) binding sites, $PBGS_{E.\ coli}$ was dialyzed against 0.1 M TES−KOH (pH 7.0), 10 mM βME, and 30 μM Zn(II); the final protein concentration was 20 mg/mL. Each EPR sample contained 40 μL of the protein sample and 10 μL of a Mn(II) solution, which varied the final Mn(II) concentration from 0.091 to 0.82 mM Mn(II) while maintaining the protein concentration at 0.456 mM. All EPR samples were later diluted 1:5 to yield a protein concentration of 91 μM and Mn(II) concentrations varying from 18 to 164 μM. Control spectra contained 0.1 M TES−KOH in place of the protein. Because of the unusually sharp lines of enzyme-bound Mn(II), the usual assumption that the intensity of the signal from the enzyme−Mn(II) complex is negligible compared to the intensity of the signal from $Mn(H_2O)_6^{2+}$ is not valid (Cohn & Townsend, 1954). Therefore, the stoichiometry and affinity of Mn(II) binding was estimated by fitting EPR signal amplitudes to an equilibrium binding model, where the total amplitude is the sum of the contributions from free Mn(II) and enzyme-bound Mn(II).

[3] More recently, we have adopted the use of 1 mM $MgCl_2$ in all purification buffers, which leads to improved yields. For protein purified in this manner, we find that Mg_C is slowly released during dialysis.

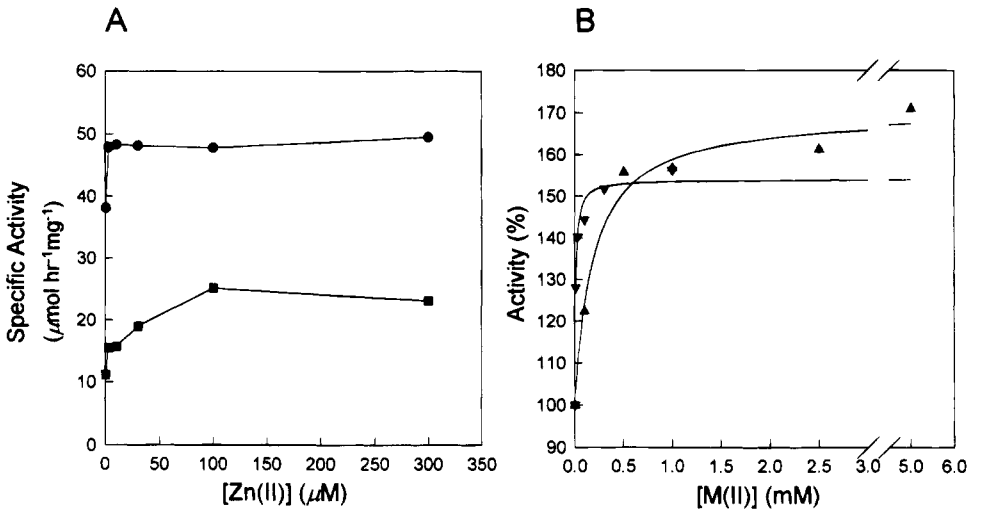

FIGURE 4: Interrelationship between Zn(II) and Mg(II) in $PBGS_{E.\ coli}$. Part A shows the requirement of $PBGS_{E.\ coli}$ for Zn(II) in the presence (●) and absence (■) of 1 mM Mg(II). Assay conditions were 0.1 M KP_i, 10 mM ALA-HCl, and 10 mM 2-mercaptoethanol (pH 6.8). Background levels of Zn(II) from buffer and substrate are ~0.4 μM. Mg(II) increases V_{max}, as well as enhances the affinity of $PBGS_{E.\ coli}$ for the required Zn(II). In the presence of Mg(II), background levels of Zn(II) are nearly sufficient to provide full activity. Part B shows the stimulation of $PBGS_{E.\ coli}$ by Mg(II) or Mn(II). The Mg(II) activation curve (▲) was acquired in 0.1 M KP_i, 100 μM Zn(II), 10 mM ALA, and 10 mM 2-mercaptoethanol (pH 6.8). The line represents a nonlinear best fit reflecting K_d = 0.19 mM and maximal activation to 170%. The Mn(II) activation curve (▼) was acquired in 0.1 M TES−KOH, 30 μM Zn, 10 mM ALA, and 10 mM 2-mercaptoethanol (pH 7.0). The line represents a nonlinear best fit reflecting K_d = 10 μM and maximal activation to 154%. Part B illustrates that Mn(II) is a good probe of the Mg_C sites with a somewhat higher affinity than Mg(II).

RESULTS

Interactive Relationship between Zn(II) and Mg(II) in the Activity of $PBGS_{E.\ coli}$. Prior to determining the kinetic constants for $PBGS_{E.\ coli}$, it was necessary to determine appropriate concentrations of Zn(II) and Mg(II). We have previously demonstrated that 1,10-phenanthroline at 0.3 mM can obliterate $PBGS_{E.\ coli}$ activity and that Zn(II), but not Mg(II), can rescue that activity from 1,10-phenanthroline inhibition (Mitchell & Jaffe, 1993). Thuz, Zn(II) is a catalytic metal. Figure 4 illustrates that, in 0.1 M KP_i (pH 7) and 10 mM ALA, 100 μM Zn(II) causes maximal activation in the absence of Mg(II). In the presence of 1 mM Mg(II), the maximal activity is significantly higher and 10 μM Zn(II) is sufficient to provide full enzyme activity. In the presence or absence of Mg(II), no significant inhibition was observed at Zn(II) concentrations as high as 0.3 mM. Figure 4B illustrates the effect of various concentrations of Mg(II) at 100 μM Zn(II); Mg(II) causes a 1.7-fold stimulation of activity with an apparent K_d of 0.2 mM. The amount of stimulation by Mg(II) varied with pH, Zn(II) concentration, and buffer [data not shown; see also Spencer and Jordan (1993)].

Kinetic constants were determined at 10 μM Zn(II) in the presence and absence of 1 mM Mg(II).[4] In the absence of Mg(II) with 10 μM Zn(II), the K_m for ALA is ~3 mM and maximal specific activity is 23 μmol h^{-1} mg^{-1}. In the presence of Mg(II) with 10 μM Zn(II), the K_m for ALA decreases to 0.3 mM, and the maximal specific activity increases to 50 μmol h^{-1} mg^{-1}. In each case, Lineweaver−Burk plots showed no evidence of cooperativity, indicating that the K_m for ALA reflects the looser binding of the two substrate molecules. In *E. coli* cytosol, where the free Mg(II) concentration is estimated to be greater than 0.3 mM (Kleme, 1976), the Mg_C site is expected to be occupied, and the K_m for ALA is comparable to that reported for mammalian PBGS (Shemin, 1972).

The Effect of Mn(II) on the Activity of $PBGS_{E.\ coli}$ Is Comparable to That Seen with Mg(II). Because manganese phosphate is of limited solubility, and Tris buffer is known to promote the oxidation of manganese, TES−KOH was chosen as buffer for the characterization of the effect of Mn(II) on the activity of $PBGS_{E.\ coli}$, for Mn(II) EPR studies, and for electrophoresis studies using Mn(II). The activity of $PBGS_{E.coli}$ in 0.1 M TES−KOH (pH 7.0) and 30 μM Zn(II) is equivalent to its activity in 0.1 M KP_i (pH 6.8) and 100 μM Zn(II). Figure 4B shows that, in TES−KOH at 30 μM Zn(II), Mn(II) causes a 1.5-fold stimulation of PBGS activity with an apparent K_d of 10 μM. On the basis of this observation, we conclude that Mn(II) is a good probe for the Mg(II) binding site of $PBGS_{E.\ coli}$.

EPR Studies of Mn(II) Bound to $PBGS_{E.\ coli}$. To investigate the stoichiometry and structure of the Mn(II) binding sites, EPR spectroscopy was used. EPR spectra of Mn(II) complexes are very sensitive to the nature of the ligands to the metal ion and to changes in the coordination sphere upon ligand substitution (Reed & Markham, 1984). When X-band EPR spectra were obtained for solutions in which the enzyme concentration exceeded the concentration of Mn(II), we observed spectra with the features shown in Figure 5A. These spectral features clearly reflect the zero field splitting of a protein-bound Mn(II) ion, rather than the simple six-line pattern of $Mn(H_2O)_6^{2+}$. The same features were observed at Mn(II)/protein ratios varying from 0.1 to 0.8, and in this range the signal intensity was proportional to the concentration of Mn(II). When the Mn(II)/protein ratio exceeded 0.8, the spectral intensity increased more rapidly and the spectra became dominated by the six-line pattern of $Mn(H_2O)_6^{2+}$. When the Mn(II)/protein ratio was 0.4, the spectrum was *ca.* ~15% as intense as the spectrum of an equal concentra-

[4] At 1 mM Mg(II) and 100 μM Zn(II), $PBGS_{E.\ coli}$ exhibits apparently normal kinetics (K_m = 1 mM, V_{max} = 50 μmol/h/μg). However, in the absence of Mg(II) at 100 μM Zn(II), the kinetic behavior resembles substrate activation. This suggests to us that Zn(II) bound in the Mg_C site may be inhibitory and that at high concentrations ALA binds the inhibitory Zn(II). Since Zn(II) bound in the Mg_C site is not physiologically significant, we did not investigate this phenomenon.

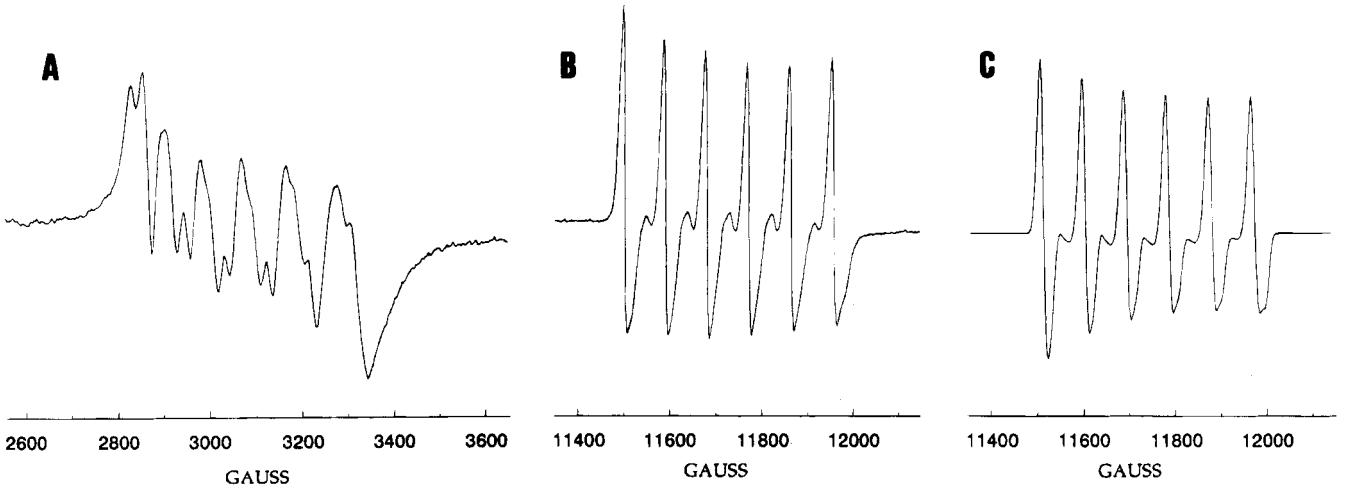

FIGURE 5: Mn(II) EPR spectra of $PBGS_{E.\ coli}$. Solutions contained 1.7 mM PBGS subunits and 0.5 mM $MnCl_2$. Part A shows the X-band EPR spectrum of the enzyme−Mn(II) complex. Spectra were recorded at 4 °C. Part B shows the Q-band EPR spectrum of the enzyme−Mn(II) complex. The spectrum was recorded at 225 K. Part C shows a computer simulation of the spectrum shown in part B. Simulation parameters were $A = 92$ G, $D = 215$ G, $E/D = 0.23$, and a Gaussian line width of 8 G.

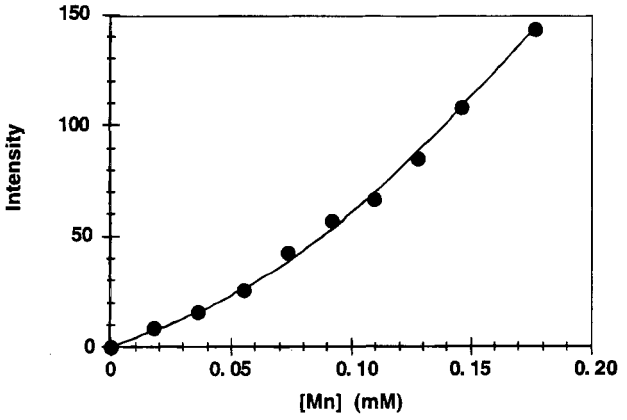

FIGURE 6: Analysis of the number of Mn(II) sites on $PBGS_{E.\ coli}$ based on the intensity of the Mn EPR signals. The signal intensity for mixtures of Mn(II) with 0.091 mM $PBGS_{E.\ coli}$ subunit rise slowly at first because the enzyme−Mn(II) complex has a broader EPR line than free Mn(II); at higher Mn(II) concentrations, as unbound Mn(II) begins to contribute, the signal intensity increases more rapidly. The line is a theoretical curve for a model of one binding site per subunit, with a dissociation constant of 16 μM and an R^2 value of 0.997. The line represents total intensity as the intensity of bound plus the intensity of free, where the former was independently determined to be 15% of the latter. The symbols are larger than the experimental error in either intensity or [Mn]. If the number of sites is allowed to vary, a best fit is obtained indicating 1.3 ± 0.3 sites per subunit.

tion of $Mn(H_2O)_6^{2+}$, which is unusually intense for a Mn(II)−protein complex; the intensity of the bound signal precluded the standard Scatchard analysis of Mn(II) binding, which assumes that the bound signal makes a negligible contribution to the total observed spectral intensity (Cohn & Townsend, 1954).

To quantify the stoichiometry of Mn(II) binding, the intensity of the EPR spectrum was monitored at numerous ratios of Mn(II) to subunit concentration, with the latter fixed at 0.091 mM, as shown in Figure 6. The results are consistent with the presence of a single Mn(II) binding site per subunit. The addition of Mg(II) to an enzyme−Mn(II) complex caused the transformation of an EPR spectrum of bound Mn(II) to one dominated by the free Mn(II) signal. This provides further evidence that Mn(II) binds to the Mg_C site (data not shown). The spectrum of the $PBGS_{E.\ coli}$−Mn(II) complex was unperturbed by the addition of either 10 mM ALA or 10 mM [1-^{13}C]ALA, suggesting that ALA does not bind directly to the Mn(II).

Because PBGS can bind two different types of Zn(II) (see Table 1), it is important to determine whether the spectrum of the PBGS−Mn(II) complex reflects one or more types of Mn(II) binding sites. Consequently, EPR spectra were recorded at Q-band (33.8 GHz), since Q-band spectra are amenable to analysis by computer simulation based on spin Hamiltonian parameters. Figure 5B shows the Q-band spectrum of the PBGS−Mn(II) complex; no changes were observed when 10 mM ALA was added. Figure 5C shows a simulation of the spectrum of Figure 5B; simulation parameters are given in the figure legend. It is apparent from the simulation that the experimental spectrum may be represented by a single set of parameters, consistent with a single type of binding site. The zero field splitting parameters $D = 215$ G and $E/D = 0.23$ indicate a fairly symmetric coordination sphere with rhombic distortion; unfortunately, due to theoretical limitations a unique interpretation of these parameters in terms of molecular structure is not yet possible (Reed & Markham, 1984). The 92 G ^{55}Mn(II) hyperfine coupling constant is characteristic of octahedrally coordinated Mn(II) with oxygen or nitrogen ligands; sulfur ligands or lower coordination numbers results in a substantial decrease in the hyperfine coupling constant (Reed & Markham, 1984). The simulations were not improved by the inclusion of the distribution in zero field splitting values commonly needed to reproduce experimental line shapes, consistent with a uniform environment of Mn(II) within the molecular ensemble and the sharp line widths observed at X-band. Thus, all indications suggest that the Mn(II) binding sites, believed to represent the Mg_C sites, are equivalent and are not near the active site of the protein. This is consistent with our observations that neither Mg(II) nor Mn(II) dramatically affected the ^{13}C NMR signals of the ^{13}C-labeled PBGS adduct formed with $PBGS_{E.\ coli}$, which had been inactivated with 5-chloro-[1,4-^{13}C]levulinic acid (Jaffe et al., 1994).

Effect of Mg(II) and Mn(II) on the Quaternary Structure of $PBGS_{E.\ coli}$. Our previous work with octameric bovine PBGS showed the quaternary structure of the protein to be extraordinarily stable. Gel filtration chromatography of $PBGS_{E.\ coli}$ on Sephacryl S-300 indicates a stable octamer that coelutes with bovine PBGS. Bovine PBGS runs as a

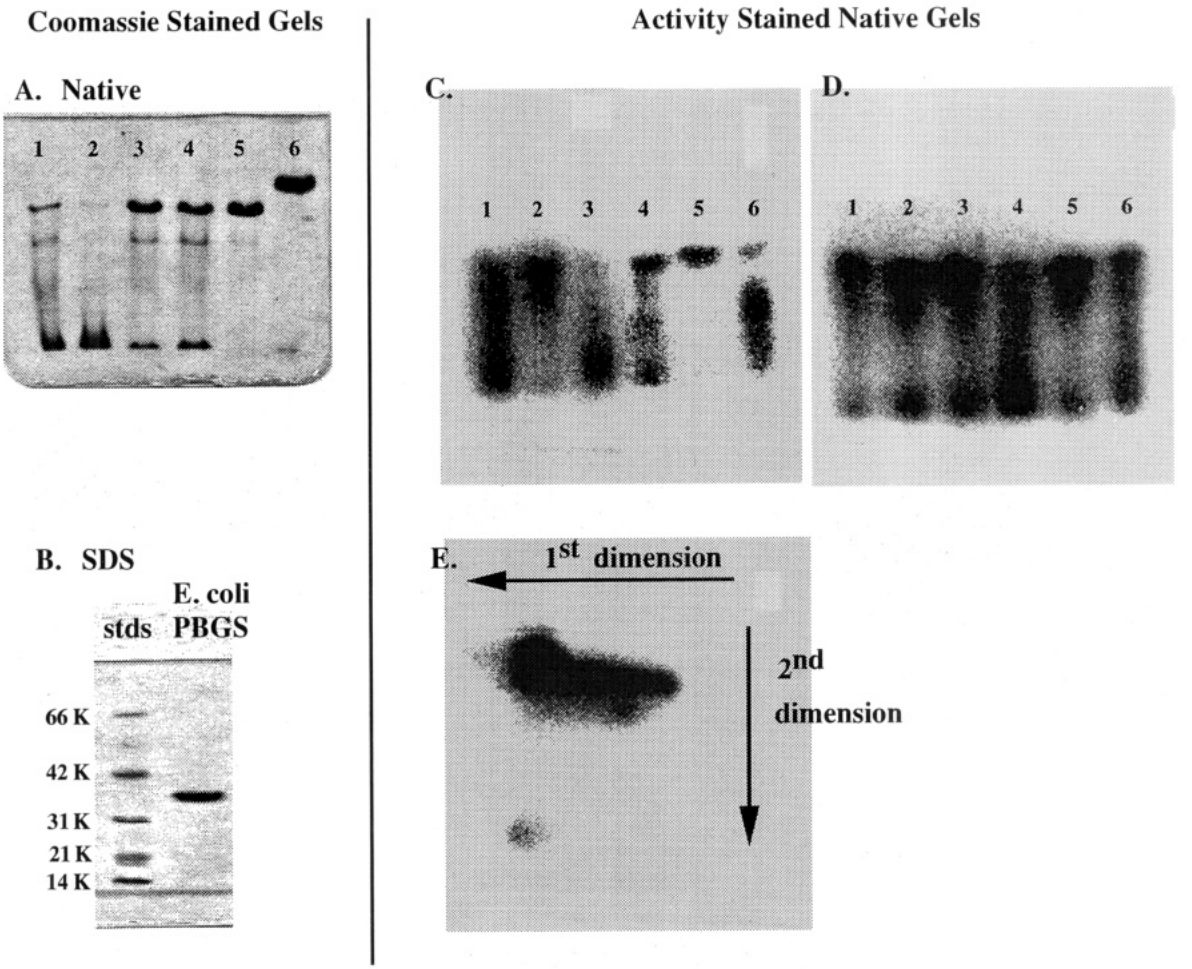

FIGURE 7: One-dimensional SDS gels and one- and two-dimensional native electrophoresis gels (Coomassie- and activity-stained). Gel A, lane 1, illustrates the dissociation of homogeneous $PBGS_{E.\ coli}$ during native gel electrophoresis. Octamers and smaller MW species are easily observed. Lane 2 illustrates the effect of preincubating the protein prior to electrophoresis in 5 mM EDTA; in this case, a larger percentage of the protein runs as the lowest MW species. Lane 3 illustrates the effect of preincubating the protein in 1 mM $MgCl_2$; a larger percentage of the protein runs as an octamer. Lane 4 shows the effect of preincubating the protein with 10 mM ALA; again, a larger percentage of the protein runs as an octamer. In lane 5, $PBGS_{E.\ coli}$ was preincubated with both 1 mM $MgCl_2$ and 10 mM ALA; only the octamer is observed. Lane 6 shows bovine PBGS, no preincubation where there is no dissociation. Gel B is an SDS gel of the protein preparation used for gel A. Lane 1 is MW markers; lane 2 is $PBGS_{E.\ coli}$. Gel C is an activity-stained native gel. The activity stain is fuzzy because product freely diffuses through the gel. Lane 1, PBGS with no preincubation; lane 2, PBGS preincubated with 1 mM $MgCl_2$; lane 3, PBGS preincubated with 5 mM EDTA. The activity staining shows that all of the protein bands in gel A are active PBGS. Lanes 4−6 were prepared like lanes 1−3, but included a second preincubation step in assay buffer (ALA, βME, and Zn(II)). The results suggest that assay buffer also prevents protein dissociation. Gel D shows the results of preincubation in assay buffer varying the components: lane 1 omits Zn(II); lane 2 omits βME, lane 3 omits Zn(II) and βME; lane 4 omits ALA; lane 5 omits nothing; and lane 6 is a control with no preincubation step. The omission of ALA results in the greatest amount of dissociation (lane 4). Gel E is a two-dimensional gel. The first dimension was run with no preincubation, as per gels A and C, lane 1, or gel D, lane 6. Prior to running the second dimension, the gel strip was soaked in complete assay mixture.

single low-mobility band on native acrylamide electrophoresis (Figure 7A, lane 6). In contrast, native gel electrophoresis of homogeneous $PBGS_{E.\ coli}$ results in multiple bands that vary in intensity, depending upon the age and history of the protein sample (Figure 7A, lane 1); SDS−PAGE shows the *E. coli* protein to be homogeneous (Figure 7B). No significant dissociation of the *E. coli* enzyme could be observed by gel filtration chromatography under a variety of buffer conditions, including Tris−glycine, which is the buffer present in the electrophoresis experiments. Dissociation of native proteins under nondenaturing electrophoresis is uncommon but not unprecedented (Lee et al., 1991) and can be used as a tool to identify elements important to subunit interactions.

One- and two-dimensional native PhastGels were used to evaluate the factors that affect protein dissociation/association. Figure 7A,C, lanes 1, illustrates Coomassie-stained and activity-stained native gels of a sample of $PBGS_{E.\ coli}$. Enzymatic activity is present in all species, as evidenced by the smear of activity through all protein bands. Preincubation of the gel sample in 1 mM $MgCl_2$ (Figure 7A, lane 3, and Figure 7C, lane 2) inhibits dissociation. Preincubation of the gel sample in 5 mM EDTA (Figure 7A, lane 2, and Figure 7C, lane 3) potentiates dissociation. These results indicate that Mg(II) promotes the stability of the octamer. Identical results were obtained with preincubation using 1 mM Mn(II) instead of Mg(II). Octamer stability can be further enhanced by the addition of substrate to assay buffer. Lanes 4−6 of Figure 7C follow the protocol of lanes 1−3 with the first preincubation, followed by a second preincubation in assay mix (ALA, Zn(II), and βME) prior to electrophoresis. In all cases, the lanes with samples preincubated in assay mix show less of the low molecular weight species than the corresponding lanes that lacked the second preincubation step. Thus, Figure 7C illustrates that assay mix potentiates the quaternary structure-stabilizing effect of

Mg(II) and protects the enzyme from the destabilizing effects of EDTA. To address whether it is the ALA or other assay mix components that promote retention of the octameric structure, Figure 7D illustrates an activity-stained native gel in which the preincubation included no additives (lane 6), assay mix (lane 5), assay mix without ALA (lane 4), ALA alone (lane 3), assay mix without βME (lane 2), and assay mix without Zn(II) (lane 1). The staining pattern indicates that the substrate, and not Zn(II) or βME, stabilizes the octamer. Figure 7A illustrates a Coomassie-stained gel that confirms these conclusions (see figure legend).

Two-dimensional gels were used to determine whether the lower MW species were catalytically active or whether reassociation of the various aggregation states to octamer occurred within the gel matrix. Figure 7E illustrates an activity-stained two-dimensional gel. The first dimension was run with no preincubation and resulted in a lane similar to lanes 1 of Figure 7A,C and lane 6 of Figure 7D. The gel strip was then soaked for 10 min in assay mix and placed atop a second gel for electrophoresis in the second dimension. Although bands running on the diagonal are observed, indicating a lack of reassociation, most species were converted to a high molecular weight species, indicating that octamer formation can occur in the gel matrix. Consequently, these experiments cannot assess whether the octamer is the only fully functional form of PBGS or whether smaller units are also catalytically active.

DISCUSSION

Our current knowledge of PBGS reveals a highly conserved metalloprotein, with some species-dependent variation in metal ion usage that can be described by a model including three types of metal ions, whose sites are denoted A, B, and C (see Table 1). Zn_A and Zn_B appear to be common to mammalian, fungal, and at least some bacterial PBGSs. Zn_A is catalytically essential in mammalian PBGS and thus is presumed common to all PBGSs. Although the activity of some PBGS species does not respond to the addition of Zn(II) or chelators, no PBGS has yet been proven to be devoid of Zn(II). The functional significance of Zn_B has yet to be elucidated, although one possibility has been proposed (Jaffe et al., 1994). The cysteine-rich putative Zn_B binding site common to mammalian, yeast, and *E. coli* PBGS is replaced by an aspartate-rich site in plant PBGS, which is illustrated in Figure 2 and has been proposed as a Mg(II) binding site (Boese et al., 1991; Jaffe, 1993). In plants, Mg_B appears to fill the yet cryptic role of Zn_B and has been proposed to be essential to activity (Jaffe et al., 1994). Mg_C appears to be common to plant and some bacterial PBGSs, but is not present in mammalian PBGS. We have analyzed the PBGS sequences for a putative Mg_C binding site, which is illustrated in Figure 3. The present results show that Mg_C is an allosteric activator of $PBGS_{E.\ coli}$ and serves to facilitate maintenance of the multimeric structure of the protein. The latter observation suggests that the C sites are at subunit interfaces.

The allosteric effect of Mg_C enhances both substrate and Zn(II) binding, as well as the turnover rate. The K_m for ALA is reduced by ~10-fold, the Zn(II) affinity is increased by at least 10-fold, and the turnover number is increased by 2-fold. Because Mg_C appears to stabilize subunit interactions at locations distinct from the active site, this suggests that motion between subunits may be part of the catalytic cycle of PBGS. The lack of the Mg_C site in mammalian PBGS is somehow compensated for with regard to quaternary structural stability, a reasonably tight K_m for ALA (~0.15 mM), and a high affinity for Zn(II) (<0.1 and 5 μM) (Jaffe et al., 1992). However, the maximal velocity of the mammalian protein is only comparable to that seen for the *E. coli* protein in the absence of Mg(II), and no allosteric effector is known for the mammalian protein.

The EPR spectrum of the PBGS−Mn(II) complex shows a single type of binding site, with a stoichiometry of eight per octamer; Mn(II) is most likely octahedrally coordinated to oxygen and/or nitrogen ligands.[5] The eight equivalent Mn(II) sites, believed to represent the Mg_C sites, are in sharp contrast to the two sets of four inequivalent Zn_A and Zn_B sites, the latter two of which are implicated to be at the four active sites (Jaffe et al., 1992, 1994). The lack of discernible spectral alterations when ALA binds suggests that ALA is not directly coordinated to the Mn(II), implying that Mn(II) is an allosteric activator, not located at the active site. The presence of four active sites per PBGS octamer suggests that the dimer is the fundamental functional unit, and small angle X-ray diffraction data support this model (Pilz et al., 1988). Because both substrate and/or Mg(II) promote octamer formation, this work was unable to address the activity of smaller species such as the dimer. One can build a model of a homooctameric protein in which there are eight equivalent subunit−subunit interfaces (*e.g.*, the Mg_C binding sites) that are separate from the four other equivalent subunit−subunit interfaces, which represent the active sites (*e.g.*, the putative locations of Zn_A and Zn_B). One such model is illustrated in Figure 8 and discussed in the legend.

There is a general similarity between *E. coli* and plants in the early steps of tetrapyrrole biosynthesis. The PBGS substrate, ALA, is synthesized in plants, *E. coli*, and some other bacteria directly from glutamic acid in a three-enzyme pathway that uses glutamyl-t-RNA as a cofactor (Mayer et. al., 1987). In yet other bacteria, fungi, and animals, ALA derives from the condensation of succinyl-CoA and glycine. Sequence analysis shows a closer relationship between plant and *E. coli* PBGS than exists between mammalian and *E. coli* PBGS (Kaczor et al., 1994; Mitchell & Jaffe, 1993). It follows that Mg_C may be common to $PBGS_{E.\ coli}$ and plant PBGS. A significant difference between $PBGS_{E.\ coli}$ and plant PBGS lies in the use of Zn_B *vs* Mg_B. It has been suggested that the high affinity of Zn(II) for chlorophyll precursors was the evolutionary driving force selecting against a chloroplast-located PBGS with a low-affinity Zn_B site (S. Beale, personal communication).

The presence of as many as three different types of metal binding sites on PBGS confounds the interpretation of inhibition by metal ion chelators. One confounding factor is the preference of the protein for different metal ions at different sites (*e.g.*, Zn_A, Zn_B or Mg_B, and Mg_C or no C site) and the affinities of metal ions for these sites. The second confounding factor is the binding preference of the chelator. For instance, EDTA preferentially binds ions that prefer

[5] Preliminary three pulse electron spin echo envelope modulation (ESEEM) spectra of the $PBGS_{E.\ coli}$ Mn(II) complexes do not show modulations due to ^{14}N in the presence or absence of substrate, nor to ^{13}C when a complex with [1-^{13}C]ALA was examined. This is consistent with a model in which all ligands to the Mn(II) are oxygen, none of which come from ALA. R. LoBrutto, personal communication.

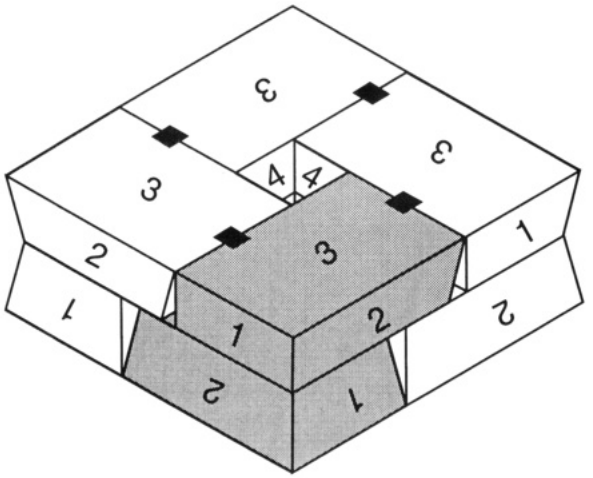

FIGURE 8: Schematic model of $PBGS_{E.\ coli}$ octamer consistent with four active sites and eight equivalent Mg_C sites. Each subunit is illustrated as a rectangular box with six distinct faces, 1−6. One functional dimer is shaded. The subunits are arranged such that faces 1−3 lie on the outside of the octamer. Faces 3 make up the top and the bottom of the octamer, faces 1 and 2 make up the sides. In all cases, 1 and 2 are side by side and on top of faces 2 and 1, which are rotated 180°. All faces 4 (opposite face 2) are flush against faces 5 (which are opposite face 1 and not visible in Figure 8). There are eight face 4 to face 5 interfaces, four which are marked with a ■ where the interface plane intersects the top of the octamer. These eight face 4 to face 5 planes represent the eight equivalent Mg_C binding sites. They are not integral to the dimer (shaded) that makes the active site. Faces 6 (opposite face 3 and not visible in Figure 8) meet in a plane that bisects the molecule. Each face 6 abuts against another face 6 that is rotated 270° relative to the first. There are four of these face 6 to face 6 interfaces; they represent the four active sites, and they lie along the midsection of the functional dimer. Each active site binds two spatially inequivalent substrate molecules and one of each type of Zn(II), Zn_A and Zn_B. We have already presented a model in which some of the ligands to Zn_A and all of the ligands to Zn_B may derive from the same region of the protein in a mutually exclusive fashion (Jaffe et al., 1992; Jaffe, 1993). There is no significance to the rectangular shape of each subunit; the inequivalent sizes of faces 1−3 are strictly for illustrative purposes.

octahedral coordination, such as Mg(II) and Mn(II), while 1,10-phenanthroline has a higher affinity for Zn(II) than for Mg(II). Nevertheless, at high enough chelator concentrations, this selectivity is lost. The third confounding factor is the various roles of the metal ions at sites A, B, and C. Consequently, past conclusions drawn on the results of PBGS inhibition, particularly by EDTA, may require reevaluation.

In summary, we conclude that $PBGS_{E.\ coli}$ binds eight structurally equivalent Mg_C ions that do not coordinate ALA directly and probably are not at the active sites. The Mg_C's are allosteric activators of $PBGS_{E.\ coli}$ and they also play a role in maintaining the octameric structure of the protein.

ACKNOWLEDGMENT

The authors are grateful to Dr. David Ash of Temple University School of Medicine for acquiring the Q-band EPR spectra and to Dr. Robert Petrovich for insightful discussions.

REFERENCES

Bishop, T. R., Frelin, L. P., & Boyer, S. H. (1986) *Nucleic Acids Res. 14*, 10115.

Bishop, T. R., Hodes, Z. I., Frelin, L. P., & Boyer, S. H. (1989) *Nucleic Acids Res. 17*, 1775.

Boese, F., Spano, A. J., Li, T., & Timko, M. J. (1991) *J. Biol. Chem. 266*, 17060−17066.

Bröckl, G., Berchtold, M., Behr, M., & König, H. (1992) *Gene 119*, 151−152.

Chauhan, S., & O'Brian, M. R. (1993) *J. Bacteriol. 175*, 7222−7227.

Cohn, M., & Townsend, J. (1954) *Nature 173*, 1090.

Dent, A. J., Beyersmann, D., Block, C., & Hasnain, S. S. (1990) *Biochemistry 29*, 7822−7828.

Echelard, Y., Dymetryszn, T., Drolet, M., & Sasarman, A. (1988) *Mol. Gen. Genet. 214*, 503−508.

Hannson, M., Rutberg, L., Schroder, I., & Hederstedt, L. (1991) *J. Bacteriol. 173*, 2590−2599.

Jaffe, E. K. (1993) *Comm. Inorg. Chem. 15*, 67−93.

Jaffe, E. K., Abrams, W. R., Kaempfen, K. X., & Harris, K. A. (1992) *Biochemistry 31*, 2113−2123.

Jaffe, E. K., Volin, M., Myers, C. B., & Abrams, W. R. (1994) *Biochemistry 33*, 11554−11562.

Jordan, P. M. (1991) in *Biosynthesis of Tetrapyrroles*, *New Comprehensive Biochemistry* (Jordan, P. M., Volume Ed.; Neuberger, A., & van Deenen, L. M., Series Eds.) Vol. 19, pp 1−61, Elsevier, Amsterdam.

Kaczor, C. M., Smith, M. W., Sangwan, I., & O'Brian, M. R. (1994) *Plant Physiol. 104*, 1411−1417.

Kleme, J. H. (1976) *Z. Naturforsch. Teil C 31*, 544−550.

Lee, B., Berka, R. M., & Tabita, F. R. (1991) *J. Biol. Chem. 266*, 7417−7422.

Li, J. M., Russell, C. S., & Cosloy, S. D. (1989) *Gene 75*, 177−184.

Liedgens, W., Grützman, R., & Schneider, H. A. W. (1980) *Z. Naturforsch. 35c*, 958−962.

Lingner, B., & Kleinschmidt, T. A. W. (1983) *Z. Naturforsch. 38*, 1059−1061.

Markham, G. D., Myers, C. B., Harris, K. A., Jr., Volin, M., & Jaffe, E. K. (1993) *Protein Sci. 2*, 71−79.

Mauzerall, D., & Granick, S. (1956) *J. Biol. Chem. 219*, 435−446.

Mayer, S. M., Beale, S. I., & Weinstein, J. D. (1987) *J. Biol. Chem. 262*, 12541−12549.

Mitchell, L. W., & Jaffe, E. K. (1993) *Arch. Biochem. Biophys. 300*, 169−177.

Myers, A. M., Crivellone, M. D., Koerner, T. J., & Tzageloff, A. (1987) *J. Biol. Chem. 262*, 16822−16829.

Pilz, I., Schwarz, E., Vuga, M., & Beyersmann, D. (1988) *Biol. Chem. Hoppe-Seyler 369*, 1099−1103.

Prasad, D. D. K., Singh, N., Datte, K., & Prasad, A. R. K. (1988) *Biochem. Int. 17*, 87−102.

Reed, G. H., & Markham, G. D. (1984) *Biological Magnetic Resonance* (Reuben, J., & Berliner, L. J., Eds.) Vol. 6, pp 73−142, Plenum Press, New York.

Schaumburg, A., Schneider-Poetsch, H. A. W., & Eckerskorn, C. (1992) *Z. Naturforsch. Teil C 47*, 77−84.

Shemin, D. (1972) *The Enzymes* (Boyer, P. D., Ed.) Vol. 7, p 232, Academic Press, San Diego.

Shemin, D., & Russell, C. S. (1954) *J. Am. Chem. Soc. 75*, 4873.

Shibata, H., & Ockiai, H. (1977) *Plant Cell Physiol. 18*, 421−429.

Spencer, P., & Jordan, P. M. (1993) *Biochem. J. 290*, 279−287.

Wetmur, J. G., Bishop, D. F., Cantelmo, D., & Desnick, R. J. (1986) *Proc. Natl. Acad. Sci. U.S.A. 83*, 7703−7707.

BI940749K